

Supporting Information

Fe_xNi_y/CeO₂ Loaded on N-doped Nanocarbon as an Advanced Bifunctional Electrocatalyst for the Overall Water Splitting

Lulu Chen,^{‡a} Haeseong Jang,^{‡b} Min Gyu Kim,^c Qing Qin,^{*a} Xien Liu,^{*a}
and Jaephil Cho^{*b}

^aState Key Laboratory Base of Eco-Chemical Engineering, College of Chemical Engineering, College of Chemistry and Molecular Engineering, Qingdao University of Science and Technology, Qingdao, 266042, P. R. China

^bDepartment of Energy Engineering and School of Energy and Chemical Engineering, Ulsan National Institute of Science and Technology (UNIST), Ulsan 689-798, South Korea

^cBeamline Research Division, Pohang Accelerator Laboratory (PAL) Pohang 790-784 (Korea)

List of contents

1. Chemicals	S4
2. Synthesis Method	S4
3. Electrochemical Measurements	S4
Fig. S1 The distribution of CeO ₂ , Fe ₁₉ Ni, and Fe _{0.64} Ni _{0.36} nanoparticles on the carbon substrate.	S6
Fig. S2 The EDS spectrum of the prepared Fe _x Ni _y /CeO ₂ /NC.	S7
Fig. S3 The XPS survey spectrum of the Fe _x Ni _y /CeO ₂ /NC catalysts.	S8
Fig. S4 The comparison of the binding energies of O 1s, Fe 2p and Ni 2p in Fe _x Ni _y /CeO ₂ /NC and Fe-Ni/NC: a) O 1s, b) Ni 2p, c) Fe 2p.	S9
Fig. S5 Raman spectrum of Fe _x Ni _y /CeO ₂ /NC.	S10
Fig. S6 a) Cyclic voltammograms recorded for a Fe _x Ni _y /CeO ₂ /NC electrode in the approximate region of 0.1-0.2 V vs. RHE at various scan rates for the purpose of determining the double layer capacitance. b) Plot showing the extraction of the double-layer capacitance (C _{dl}) of Fe _x Ni _y /CeO ₂ /NC, Fe-Ni/NC, Fe-Ce/NC, Ni-Ce/NC.	S11
Fig. S7 The XRD patterns of the Fe _x Ni _y /CeO ₂ /NC catalysts before test and after HER and OER testing.	S12
Fig. S8 High resolution XPS spectra of the as-synthesized Fe _x Ni _y /CeO ₂ /NC composite. a) Ce 3d before and after OER testing. b) Ce 3d before and after HER testing.	S13
Figure S9 XPS spectra of the as-synthesized Fe _x Ni _y /CeO ₂ /NC composite. a) Fe 2p, and b) Ni 2p before and after OER testing. c) Fe 2p and d) Ni 2p before and after HER testing.	S14

Table S1 The change of the relative contents of Ce^{3+} and Ce^{4+} in the hybrid catalyst before and after HER/OER testing.	S13
Table S2 Comparison of catalytic properties of $\text{Fe}_x\text{Ni}_y/\text{CeO}_2/\text{NC}$ and reported catalyst HER in alkaline electrolyte.	S15
Table S3 Comparison of catalytic properties of $\text{Fe}_x\text{Ni}_y/\text{CeO}_2/\text{NC}$ and reported catalyst OER in alkaline electrolyte.	S16
Table S4 Comparison of catalytic performance of $\text{Fe}_x\text{Ni}_y/\text{CeO}_2/\text{NC}$ for two-electrode water splitting to reported catalysts.	S17

Chemicals

Melamine Monomer ($C_3H_6N_6$) was purchased from TCI (Shanghai) Development Co. Ltd. $Fe(NO_3)_3 \cdot 9H_2O$ (MW: 404) and $Ce(NO_3)_3 \cdot 6H_2O$ (MW: 434.22) were obtained from MACKLIN Co., Ltd. $Ni(NO_3)_2 \cdot 6H_2O$ (MW: 290.79), Nafion (5 wt%), commercial Pt/C (20 wt%) catalyst and commercial IrO_2 catalyst were ordered at Sigma – Aldrich Co. Ltd. All of the reagents were purchased and directly used without further purification.

Synthesis Method

Synthesis of $Fe_xNi_y/CeO_2/NC$ catalyst: In a typical synthesis procedure, 1.0 g of $C_3H_6N_6$ was added into 40 mL of deionized water under vigorously stirring to form a homogeneous solution. Then, 0.1 g of $Fe(NO_3)_3 \cdot 9H_2O$, 0.1 g of $Ce(NO_3)_3 \cdot 6H_2O$ and 0.1 g of $Ni(NO_3)_2 \cdot 6H_2O$ were successively added to the above solution and continuously stirred for 12 h at room temperature. Afterward, the emulsion-like solution was heated to 70 °C to remove the most solvent and then further dried in vacuum at 80 °C for 2 h. After that, the obtained black power was annealed at 700 °C for 2 h under an Ar atmosphere with a gas flow rate of 150 mL min⁻¹. When cooled to room temperature at Ar atmosphere, the obtained products were collected and directly used for electrochemical tests.

Synthesis of $Fe-Ni/NC$, $Fe-Ce/NC$, $Ni-Ce/NC$ catalysts: The synthetic methods of $Fe-Ni/NC$, $Fe-Ce/NC$, and $Ni-Ce/NC$ catalysts are similar with that of $Fe_xNi_y/CeO_2/NC$ catalyst, except without the addition of $Ce(NO_3)_3 \cdot 6H_2O$ or $Fe(NO_3)_3 \cdot 9H_2O$ or $Ni(NO_3)_2 \cdot 6H_2O$ into the reaction systems.

Electrochemical Measurements

The electrocatalytic hydrogen evolution reaction (HER) and oxygen evolution reaction (OER) performances of the prepared catalysts were tested in a 1.0 M KOH

electrolyte using a traditional three-electrode system, using a graphite rod and a reversible hydrogen electrode as the counter electrode and the reference electrode, respectively. The working electrode was prepared by loading 5 μL of the catalyst ink on a glass carbon (GC, 3 mm) electrode. The catalyst ink was obtained by dispersing 3.0 mg of catalyst powders and 60 μL of Nafion (5 wt%) in 0.3 mL of ultra-pure water and 0.15 mL of ethanol by ultrasonic for 15 min. The polarization curves were measured at a scan rate of 5 mV s^{-1} . All the data are originally obtained without iR compensation. The electrocatalytic stability of the catalysts was investigated by the chronoamperometry method at a constant potential of -0.24 V (vs. RHE) for HER and 1.47 V (vs RHE) for OER. The electrochemically active surface area (ECSA) of the $\text{Fe}_x\text{Ni}_y/\text{CeO}_2/\text{NC}$ is systematically evaluated by the electrochemical double-layer capacitance (C_{dl}) using CVs with varied scan rates in the potential range of 0.1 V – 0.2 V (vs RHE).

Overall water splitting. The overall water splitting performance of the $\text{Fe}_x\text{Ni}_y/\text{CeO}_2/\text{NC}$ catalyst was evaluated in a self-assembled two-electrode setup with the catalyst as both the anode and cathode. The Ni foam (1×1 cm) with loading 0.2 mg of catalyst as the working electrode. The polarization curves were recorded at a scan rate of 5 mV s^{-1} . The applied voltage was fixed at 0.8 V - 2.0 V. The durability test was investigated by the chronoamperometry method at a constant voltage of 1.70 V for 24 h.

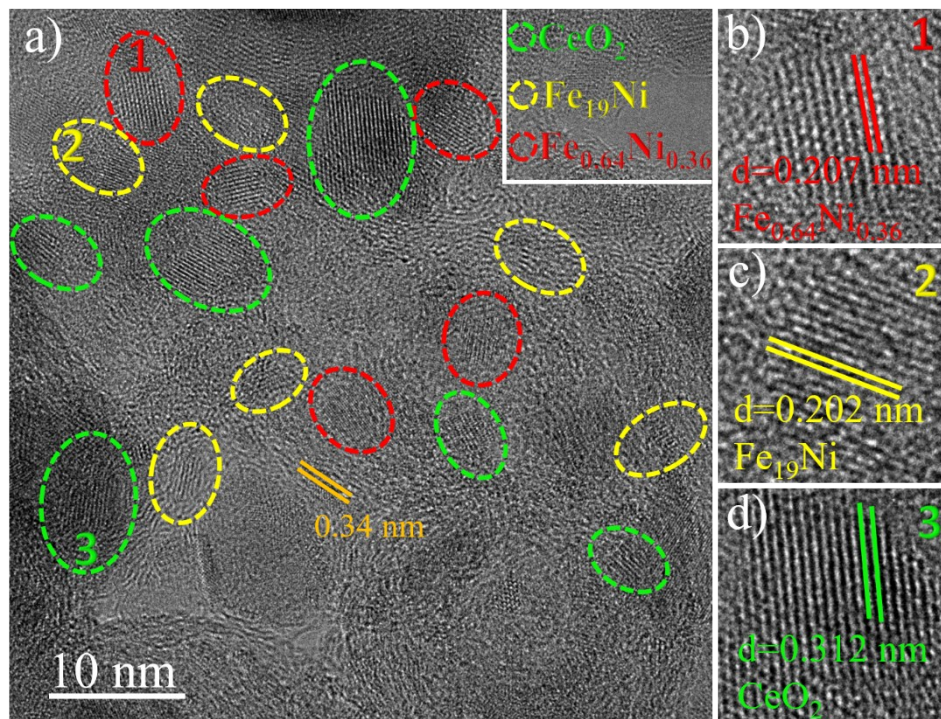


Fig. S1 The distribution of CeO_2 , Fe_{19}Ni , and $\text{Fe}_{0.64}\text{Ni}_{0.36}$ nanoparticles on the carbon substrate.



Fig. S2 The EDS spectrum of the prepared $\text{Fe}_x\text{Ni}_y/\text{CeO}_2/\text{NC}$.

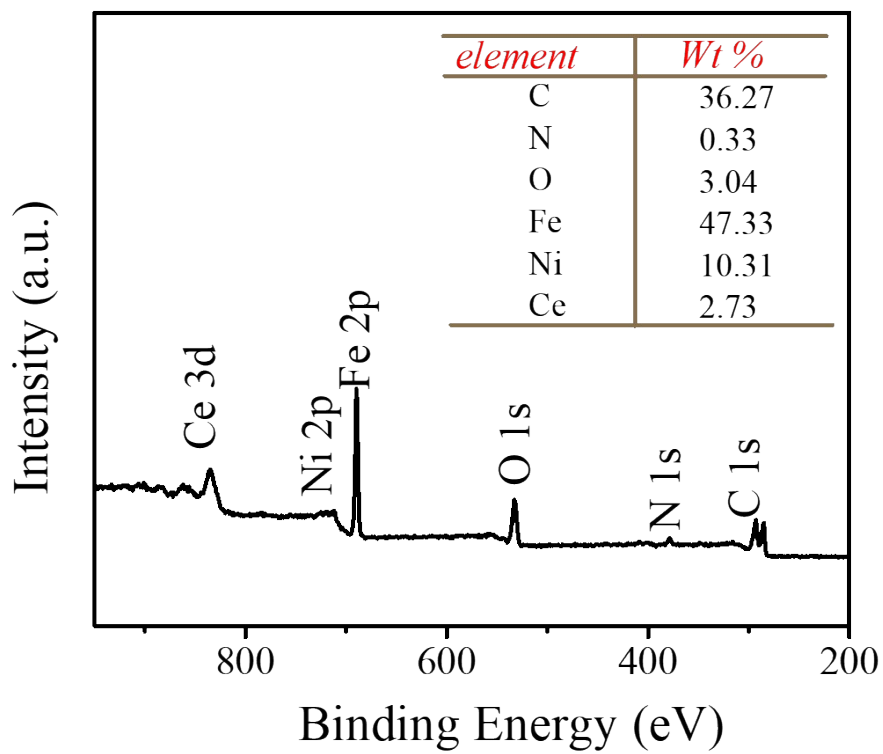


Fig. S3 The XPS survey spectrum of the $\text{Fe}_x\text{Ni}_y/\text{CeO}_2/\text{NC}$ catalysts.

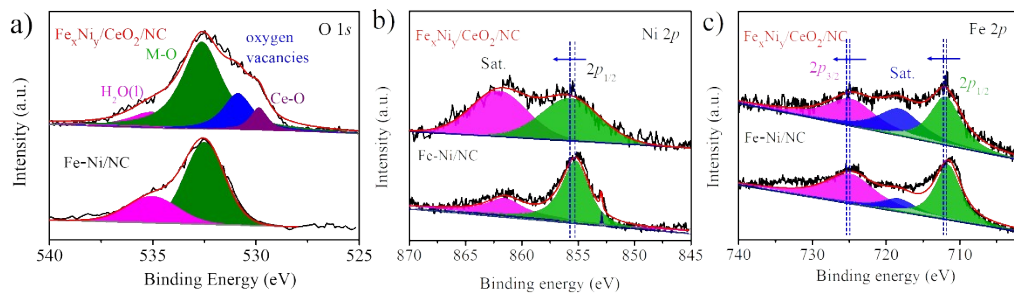


Fig. S4 The comparison of the binding energies of O 1s, Fe 2p and Ni 2p in $\text{Fe}_x\text{Ni}_y/\text{CeO}_2/\text{NC}$ and Fe-Ni/NC : a) O 1s, b) Ni 2p, c) Fe 2p.

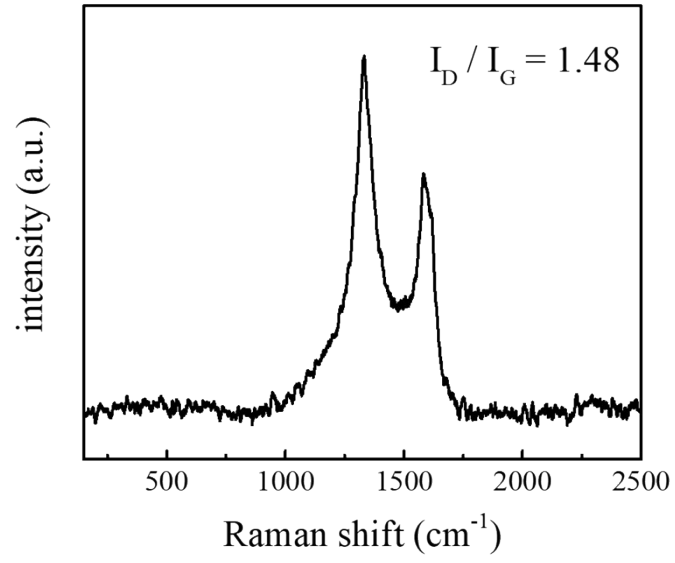


Fig. S5 Raman spectrum of Fe_xNi_y/CeO₂/NC.

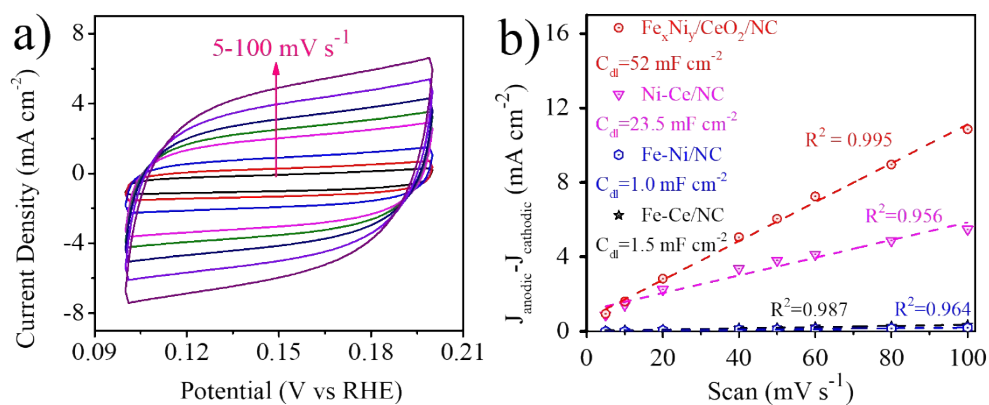


Fig. S6 a) Cyclic voltammograms recorded for a $\text{Fe}_x\text{Ni}_y/\text{CeO}_2/\text{NC}$ electrode in the approximate region of 0.1-0.2 V vs. RHE at various scan rates for the purpose of determining the double layer capacitance. b) Plot showing the extraction of the double-layer capacitance (C_{dl}) of $\text{Fe}_x\text{Ni}_y/\text{CeO}_2/\text{NC}$, Fe-Ni/NC , Fe-Ce/NC , Ni-Ce/NC .

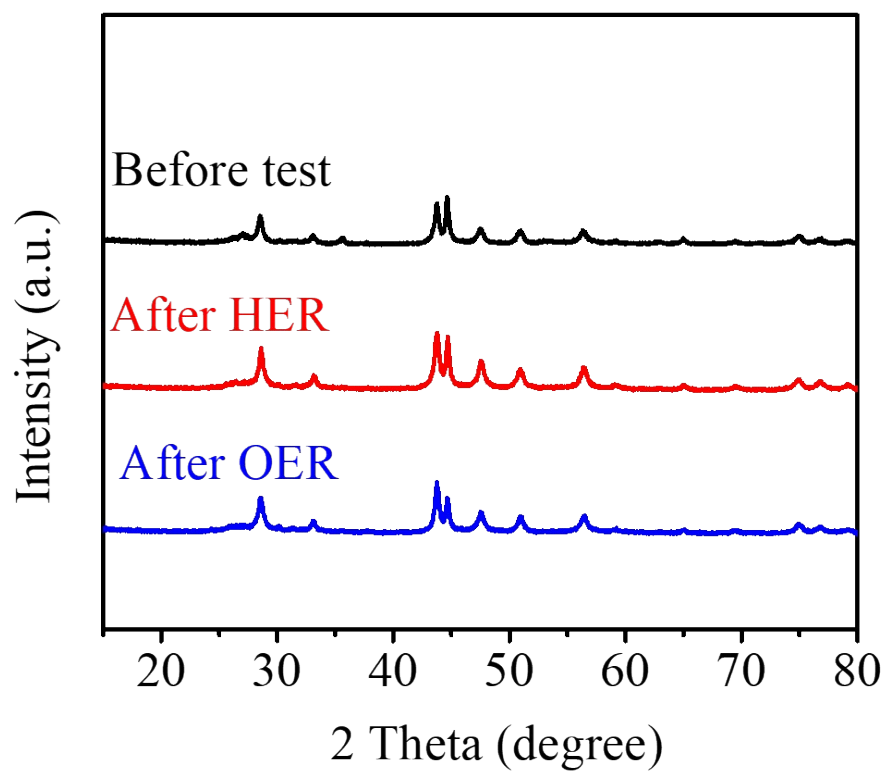


Fig. S7 The XRD patterns of the $\text{Fe}_x\text{Ni}_y/\text{CeO}_2/\text{NC}$ catalysts before and after HER and OER testing.

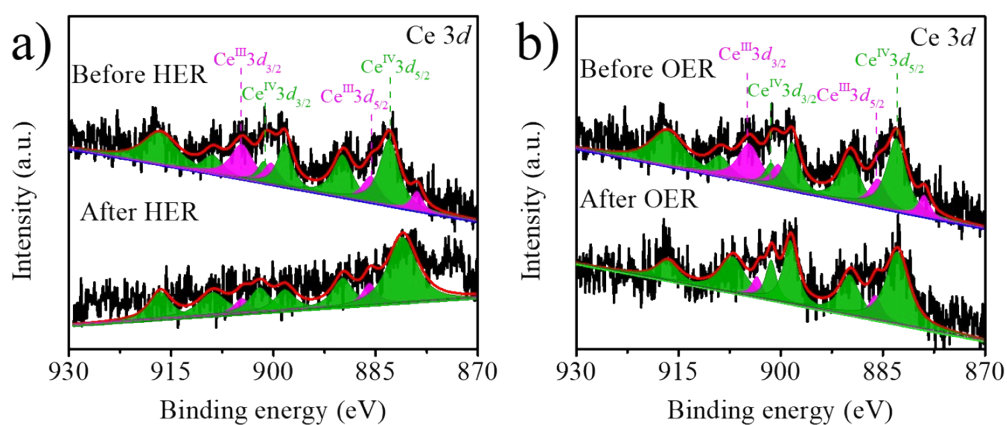


Fig. S8 High resolution XPS spectra of the as-synthesized $\text{Fe}_x\text{Ni}_y/\text{CeO}_2/\text{NC}$ composite.

a) Ce 3d before and after OER testing. b) Ce 3d before and after HER testing.

Table S1 The change of the relative contents of Ce^{3+} and Ce^{4+} in the hybrid catalyst before and after HER/OER testing.

Condition	Percentage of Ce^{3+}	Percentage of Ce^{4+}
Before test	28.3%	71.7%
After HER	10.26%	89.74%
After OER	9.4%	90.6%

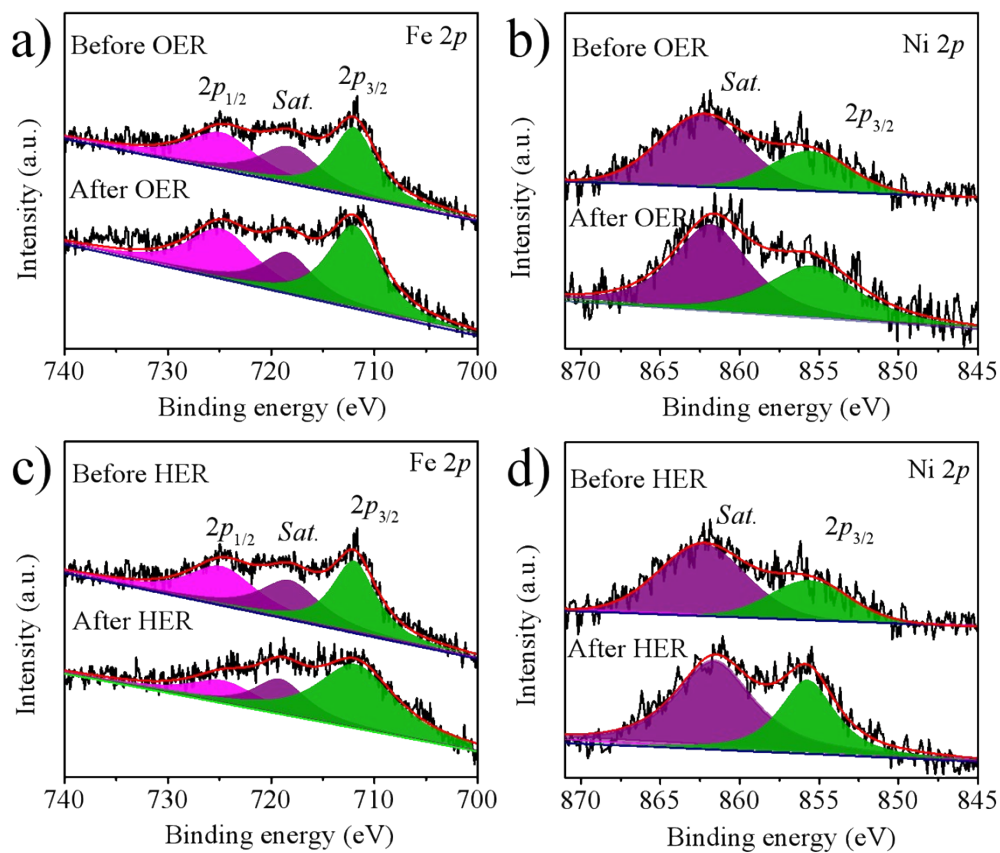


Fig. S9 XPS spectra of the as-synthesized $\text{Fe}_x\text{Ni}_y/\text{CeO}_2/\text{NC}$ composite. a) Fe 2p, and b) Ni 2p before and after OER testing. c) Fe 2p and d) Ni 2p before and after HER testing.

Table S2 Comparison of catalytic properties of Fe_xNi_y/CeO₂/NC and reported catalyst
HER in alkaline electrolyte

Catalysts	Catalyst loading (mg cm ⁻²)	Overpotentia@j (mV@10 mA cm ⁻²)	Electrolyte	Ref.
FeNi&CeO₂/C	0.41	240	1.0 M KOH	This work
NiFe LDH-NS@DG10	0.28	300	1.0 M KOH	1
EG/Co_{0.85}Se/Ni Fe-LDH	4.00	~260	1.0 M KOH	2
Ni₃FeN-NPs	0.35	158	1.0 M KOH	3
NiCoP/rGO	0.15	209	1.0 M KOH	4
Ni₃S₂/NF	N/A	223	1.0 M KOH	5
FeP NAs/CC	N/A	218	1.0 M KOH	6
NCNT/MnO-(MnFe)₂O₃	0.14	212	1.0 M KOH	7

Table S3 Comparison of catalytic properties of Fe_xNi_y/CeO₂/NC and reported catalyst OER in alkaline electrolyte

Catalysts	Catalyst loading	Overpotentia@j (mV@10 mA cm ⁻²)	Electrolyte	Ref.
FeNi&CeO₂/C	0.41	240	1.0 M KOH	This work
NiFe LDH-NS@DG10	0.28	210	1.0 M KOH	1
FeCoNi-2	0.32	325	1.0 M KOH	8
Porous Ni-P	N/A	~312	1.0 M KOH	9
NiFe LDH/NGF	0.25	340	0.1 M KOH	10
NiCo₂O₄	0.28	380	1.0 M KOH	11
Ni₃FeN/r-GO	0.50	279	1.0 M KOH	12
NiCo₂O₄hollow microcuboids	1.00	290	1.0 M NaOH	13
NiFe LDH/r-GO	0.25	210	1.0 M KOH	14
NiFe-SW film	N/A	240	1.0 M KOH	15
NiFe-MoO_xNS	0.20	276	1.0 M KOH	16

Table S4 Comparison of catalytic performance of $\text{Fe}_x\text{Ni}_y/\text{CeO}_2/\text{NC}$ for two-electrode water splitting to reported catalysts

Catalysts	Catalyst loading	Voltage@j (V@10 mA cm ⁻²)	Catalyst support	Ref.
FeNi&CeO₂/C	0.20	1.70	NF	This work
Ni₃S₂/NF	N/A	1.76@13	NF	5
NCNT/MnO-(MnFe)₂O₃	0.21	1.71	NF	7
Ni_{0.33}Co_{0.67}S₂NWs	0.30	1.72	TF	17
NiFe LDH	N/A	1.70	NF	18
Ni₅P₄	3.5	1.70	NF	19
Co₁Mn₁CH	5.6	1.68	NF	20
Fe-Co CF	1.2 or 2.0	1.68	CFP	21
NiFe/NiCo₂O₄	N/A	1.67	NF	22
Fe-CoP/Ti	N/A	1.60	TF	23
NiCoP/Ni foam	5.0	1.77	NF	24

NF: Ni foam; CFP: carbon fiber paper; TF: Ti foil

References

1. Jia, Y.; Zhang, L.; Gao, G.; Chen, H.; Wang, B.; Zhou, J.; Soo, M. T.; Hong, M.; Yan, X.; Qian, G. J. A. M., A heterostructure coupling of exfoliated Ni–Fe hydroxide nanosheet and defective graphene as a bifunctional electrocatalyst for overall water splitting. *Advanced Materials* **2017**, *29* (17), 1700017.
2. Hou, Y.; Lohe, M. R.; Zhang, J.; Liu, S.; Zhuang, X.; Feng, X. J. E.; Science, E., Vertically oriented cobalt selenide/NiFe layered-double-hydroxide nanosheets supported on exfoliated graphene foil: an efficient 3D electrode for overall water splitting. *Energy & Environmental Science* **2016**, *9* (2), 478-483.
3. Jia, X.; Zhao, Y.; Chen, G.; Shang, L.; Shi, R.; Kang, X.; Waterhouse, G. I.; Wu, L. Z.; Tung, C. H.; Zhang, T. J. A. E. M., Ni₃FeN Nanoparticles Derived from Ultrathin NiFe-Layered Double Hydroxide Nanosheets: An Efficient Overall Water Splitting Electrocatalyst. *Advanced Energy Materials* **2016**, *6* (10), 1502585.
4. Li, J.; Yan, M.; Zhou, X.; Huang, Z. Q.; Xia, Z.; Chang, C. R.; Ma, Y.; Qu, Y. J. A. F. M., Mechanistic insights on ternary Ni²⁻_xCo_xP for hydrogen evolution and their hybrids with graphene as highly efficient and robust catalysts for overall water splitting. *Advanced Functional Materials* **2016**, *26* (37), 6785-6796.
5. Feng, L.-L.; Yu, G.; Wu, Y.; Li, G.-D.; Li, H.; Sun, Y.; Asefa, T.; Chen, W.; Zou, X. J. J. o. t. A. C. S., High-index faceted Ni₃S₂ nanosheet arrays as highly active and ultrastable electrocatalysts for water splitting. *Journal of the American Chemical Society* **2015**, *137* (44), 14023-14026.

-
6. Liang, Y.; Liu, Q.; Asiri, A. M.; Sun, X.; Luo, Y. J. A. C., Self-supported FeP nanorod arrays: a cost-effective 3D hydrogen evolution cathode with high catalytic activity. *Angewandte Chemie International Edition* **2014**, *4* (11), 4065-4069.
 7. Qin, Q.; Li, P.; Chen, L.; Liu, X., Coupling Bimetallic Oxides/Alloys and N-Doped Carbon Nanotubes as Tri-Functional Catalysts for Overall Water Splitting and Zinc–Air Batteries. *ACS Appl. Mater. Interfaces* **2018**, *10* (46), 39828-39838.
 8. Yang, Y.; Lin, Z.; Gao, S.; Su, J.; Lun, Z.; Xia, G.; Chen, J.; Zhang, R.; Chen, Q. J. A. C., Tuning electronic structures of nonprecious ternary alloys encapsulated in graphene layers for optimizing overall water splitting activity. *ACS Catalysis* **2016**, *7* (1), 469-479.
 9. Wang, X.; Li, W.; Xiong, D.; Liu, L. J. J. o. M. C. A., Fast fabrication of self-supported porous nickel phosphide foam for efficient, durable oxygen evolution and overall water splitting. *Journal of Materials Chemistry A* **2016**, *4* (15), 5639-5646.
 10. Tang, C.; Wang, H. S.; Wang, H. F.; Zhang, Q.; Tian, G. L.; Nie, J. Q.; Wei, F. J. A. M., Spatially confined hybridization of nanometer-sized NiFe hydroxides into nitrogen-doped graphene frameworks leading to superior oxygen evolution reactivity. *Advanced Materials* **2015**, *27* (30), 4516-4522.
 11. Han, L.; Yu, X. Y.; Lou, X. W. J. A. m., Formation of Prussian-Blue-Analog Nanocages via a Direct Etching Method and their Conversion into Ni–Co-Mixed Oxide for Enhanced Oxygen Evolution. *Advanced Materials* **2016**, *28* (23), 4601-4605.

-
12. Gu, Y.; Chen, S.; Ren, J.; Jia, Y. A.; Chen, C.; Komarneni, S.; Yang, D.; Yao, X. J. A. n., Electronic structure tuning in Ni₃FeN/r-GO aerogel toward bifunctional electrocatalyst for overall water splitting. *ACS Nano* **2018**, *12* (1), 245-253.
13. Gao, X.; Zhang, H.; Li, Q.; Yu, X.; Hong, Z.; Zhang, X.; Liang, C.; Lin, Z. J. A. C. I. E., Hierarchical NiCo₂O₄ Hollow Microcuboids as Bifunctional Electrocatalysts for Overall Water-Splitting. *Angewandte Chemie International Edition* **2016**, *55* (21), 6290-6294.
14. Ma, W.; Ma, R.; Wang, C.; Liang, J.; Liu, X.; Zhou, K.; Sasaki, T. J. A. n., A superlattice of alternately stacked Ni-Fe hydroxide nanosheets and graphene for efficient splitting of water. *ACS Nano* **2015**, *9* (2), 1977-1984.
15. Zhang, W.; Wu, Y.; Qi, J.; Chen, M.; Cao, R. J. A. E. M., A thin NiFe hydroxide film formed by stepwise electrodeposition strategy with significantly improved catalytic water oxidation efficiency. *Advanced Energy Materials* **2017**, *7* (9), 1602547.
16. Xie, C.; Wang, Y.; Hu, K.; Tao, L.; Huang, X.; Huo, J.; Wang, S. J. J. o. M. C. A., In situ confined synthesis of molybdenum oxide decorated nickel-iron alloy nanosheets from MoO₄²⁻ intercalated layered double hydroxides for the oxygen evolution reaction. *Journal of Materials Chemistry A* **2017**, *5* (1), 87-91.
17. Peng, Z.; Jia, D.; Al-Enizi, A. M.; Elzatahry, A. A.; Zheng, G. J. A. E. M., From water oxidation to reduction: homologous Ni-Co based nanowires as complementary water splitting electrocatalysts. *Advanced Energy Materials* **2015**, *5* (9), 1402031.
18. Luo, J.; Im, J.-H.; Mayer, M. T.; Schreier, M.; Nazeeruddin, M. K.; Park, N.-G.; Tilley, S. D.; Fan, H. J.; Grätzel, M. J. S., Water photolysis at 12.3% efficiency via

-
- perovskite photovoltaics and Earth-abundant catalysts. *Science* **2014**, *345* (6204), 1593-1596.
19. Marc, L.; Sandra, K. C.; Christian, P.; Hans-Peter, S.; Markus, A.; Menny, S. J. A. C., The Synthesis of Nanostructured Ni₅P₄ Films and their Use as a Non-Noble Bifunctional Electrocatalyst for Full Water Splitting. *Angewandte Chemie International Edition* **2015**, *54* (42), 12361-12365.
20. Tang, T.; Jiang, W.-J.; Niu, S.; Liu, N.; Luo, H.; Chen, Y.-Y.; Jin, S.-F.; Gao, F.; Wan, L.-J.; Hu, J.-S. J. J. o. t. A. C. S., Electronic and morphological dual modulation of cobalt carbonate hydroxides by Mn doping toward highly efficient and stable bifunctional electrocatalysts for overall water splitting. *Journal of the American Chemical Society* **2017**, *139* (24), 8320-8328.
21. Liu, W.; Du, K.; Liu, L.; Zhang, J.; Zhu, Z.; Shao, Y.; Li, M. J. N. E., One-step electroreductively deposited iron-cobalt composite films as efficient bifunctional electrocatalysts for overall water splitting. *Nano Energy* **2017**, *38*, 576-584.
22. Xiao, C.; Li, Y.; Lu, X.; Zhao, C. J. A. F. M., Bifunctional porous NiFe/NiCo₂O₄/Ni foam electrodes with triple hierarchy and double synergies for efficient whole cell water splitting. *Advanced Functional Materials* **2016**, *26* (20), 3515-3523.
23. Tang, C.; Zhang, R.; Lu, W.; He, L.; Jiang, X.; Asiri, A. M.; Sun, X. J. A. m., Fe-doped CoP nanoarray: a monolithic multifunctional catalyst for highly efficient hydrogen generation. *Advanced Materials* **2017**, *29* (2), 1602441.

-
24. Li, Y.; Zhang, H.; Jiang, M.; Kuang, Y.; Sun, X.; Duan, X. J. N. R., Ternary NiCoP nanosheet arrays: An excellent bifunctional catalyst for alkaline overall water splitting. *Nano Research* **2016**, *9* (8), 2251-2259.